ATM Requirement in Gene Expression Responses to Ionizing Radiation in Human Lymphoblasts and Fibroblasts

Cynthia L. Innes,[1] Alexandra N. Heinloth,[2] Kristina G. Flores,[1] Stella O. Sieber,[2] Paula B. Deming,[3] Pierre R. Bushel,[2] William K. Kaufmann,[3] and Richard S. Paules[1,2]

[1]Growth Control and Cancer Group, and [2]National Institute of Environmental Health Sciences Microarray Group, National Institute of Environmental Health Sciences, Research Triangle Park, North Carolina; [3]Department of Pathology and Laboratory Medicine, University of North Carolina at Chapel Hill School of Medicine, Chapel Hill, North Carolina

Abstract

The heritable disorder ataxia telangiectasia (AT) is caused by mutations in the *AT-mutated* (*ATM*) gene with manifestations that include predisposition to lymphoproliferative cancers and hypersensitivity to ionizing radiation (IR). We investigated gene expression changes in response to IR in human lymphoblasts and fibroblasts from seven normal and seven AT-affected individuals. Both cell types displayed ATM-dependent gene expression changes after IR, with some responses shared and some responses varying with cell type and dose. Interestingly, after 5 Gy IR, lymphoblasts displayed ATM-independent responses not seen in the fibroblasts at this dose, which likely reflect signaling through ATM-related kinases, e.g., ATR, in the absence of ATM function. (Mol Cancer Res 2006;4(3):197–207)

Introduction

Ataxia telangiectasia (AT) is an autosomal-recessive, hereditary syndrome characterized by neuronal degeneration, telangiectasias, immunodeficiencies, lymphoid cancers (1), and cell cycle checkpoint defects in cultured cells (2, 3). Individuals with AT have mutations in the gene *AT-mutated* (*ATM*). The ATM protein is a serine/threonine kinase that is activated by ionizing radiation (IR; refs. 4, 5). AT is one of a number of familial cancer syndromes in which individuals have enhanced sensitivity to DNA-damaging agents (6-8). The human genome is exposed to many forms of DNA damage and it is critical for health to maintain signaling pathways that repair such damage. IR damages DNA, eliciting cell cycle checkpoint responses to discontinue proliferation until damage is repaired. It is known that in different types of cells, different signaling pathways are activated in response to stress (9). Therefore, we compared the role of ATM signaling in response to DNA damage in human lymphoblasts and human fibroblasts using microarray technology to examine gene expression responses to exposure to IR.

Results

Because cell type can play a role in determining which signaling pathways are activated in response to cellular stress or DNA damage (9), we examined the role of ATM in signaling pathways in response to IR-induced DNA damage in human lymphoblasts and compared the results with those from a previous study of the role of ATM in human fibroblasts (10). Cultures of each cell type (lymphoblast and fibroblast) and genetic background [wild type (WT) and AT] were analyzed from multiple individuals to gain information about the ATM-dependent and ATM-independent responses while reducing the effects of individual genetic variation (11, 12). Initially, six lymphoblast cultures (three WT and three AT) and six fibroblast cultures (three WT and three AT) were exposed to 5 Gy IR (10) for a comparison of IR treatment between cell types. Subsequently, the same six lymphoblast cultures and an additional culture of each (for a total of four WT and four AT) were exposed to 1 Gy IR.

G_1 and G_2 Checkpoints Are Attenuated in AT Cultures

We have previously shown G_1 checkpoint responses to IR in fibroblasts to be strong in WT cells and attenuated in AT cells (13, 14). WT lymphoblasts in this study displayed an activation of the ATM kinase (data not shown) and the characteristic G_1 checkpoint response to DNA damage induced by IR. The AT lymphoblasts displayed a markedly attenuated G_1 checkpoint response to IR. The response of WT lymphoblasts was slightly attenuated from what we have observed previously with WT fibroblasts following similar exposures to IR (13-15).[4]

[4] Unpublished data.

Received 8/25/05; revised 1/12/06; accepted 1/26/06.
Grant support: Intramural Research Program of the NIH, National Institute of Environmental Health Sciences, and NIH grants CA81343 and ES011391 (W.K. Kaufmann).
The costs of publication of this article were defrayed in part by the payment of page charges. This article must therefore be hereby marked advertisement in accordance with 18 U.S.C. Section 1734 solely to indicate this fact.
Note: K.G. Flores is currently in Epidemiology and Cancer Prevention, MSC11-6020, 1 University of New Mexico, Albuquerque, NM 87131. P.B. Deming is currently in Department of Pathology, University of Vermont, Burlington, VT 05405.
Microarray data have been deposited in the Gene Expression Omnibus at the National Center for Biotechnology Information database (http://www.ncbi.nlm.nih.gov).The accession number is GSE3174.
Requests for reprints: Richard S. Paules, Growth Control and Cancer Group, National Institute of Environmental Health Sciences, PO Box 12233, MD D2-03, Research Triangle Park, NC 27709. Phone: 919-541-3710; Fax: 919-316-4771. E-mail: paules@niehs.nih.gov.

doi:10.1158/1541-7786.MCR-05-0154

In response to IR, WT cells delay at a G_2 checkpoint, causing a decrease in the number of cells entering mitosis. To quantify the G_2 checkpoint response in lymphoblasts, we measured the IR-induced reduction in mitosis. Mitotic cells were determined as the population of cells that showed phosphorylation of histone H3, and the relative mitotic index was expressed as the percentage of phosphohistone H3–positive cells in the irradiated population relative to the mock-treated population (Fig. 1). WT lymphoblasts displayed a strong G_2 checkpoint response with >90% reduction of the number of cells in mitosis 2 hours after 1 Gy IR, but by 6 hours after 1 Gy IR the WT cells had recovered from the G_2 delay, with mitosis at near control levels (Fig. 1). AT lymphoblasts displayed the expected attenuation of G_2 checkpoint response to IR with less inhibition of entry into mitosis at 2 hours post-IR and impaired recovery of mitosis at 6 hours (Fig. 1). However, following 5 Gy IR, both the WT and AT lymphoblasts displayed a severe and long-lasting G_2 arrest with no recovery seen after 6 hours (Fig. 1). These observations suggested that there was an ATM-independent signaling mechanism that induced G_2 delay in the AT lymphoblasts following 5 Gy IR.

We have examined G_2 checkpoint function in human fibroblasts previously; WT fibroblasts displayed an intact response, with the response in AT fibroblasts attenuated following IR (2, 14).[4] We also observed that entry into mitosis was strongly inhibited in WT fibroblasts 6 hours following 5 Gy IR but greater fractions of mitotic cells were observed in the IR-treated AT fibroblasts than WT fibroblasts (data not shown). In comparing the two cell types, the G_2 delay responses of the WT fibroblasts, WT lymphoblasts, and AT lymphoblasts treated with 5 Gy IR seemed equivalent, whereas the response of the AT fibroblasts treated with 5 Gy IR seemed to be more similar to that of the AT lymphoblasts treated with 1 Gy IR. These observations suggested that there was an ATM-independent signaling mechanism that induced G_2 delay in the AT lymphoblasts following 5 Gy IR.

To better understand the response of different cell types to IR-induced damage, we looked at gene expression changes in lymphoblasts and fibroblasts. Cells were exposed to the same dose of IR, 5 Gy, as well as a lower dose (1 Gy) for the lymphoblasts that generated a checkpoint response in the AT lymphoblasts that was more biologically similar to the response of AT fibroblasts treated with 5 Gy IR. In addition, we compared ATM-dependent and ATM-independent responses in these two cell types to IR-induced damage. We looked first at categories of biological processes affected by IR exposure as revealed by gene expression analysis and then more specifically at particular gene expression changes to focus on some of the specific responses involved in the response to IR-induced DNA damage.

Differential Gene Expression Reveals Overall Biological Responses

Genes that were significantly differentially expressed between matched IR- and mock-treated fibroblasts and lymphoblasts were identified based on a confidence level approach or mixed linear model ANOVA approach and are shown in Table 1. To gain insight into the biological processes affected by exposure to IR in either an ATM-dependent or ATM-independent manner, and to determine potential cell type differences, we did an analysis of differentially expressed genes (Table 1) with respect to their Gene Ontology Biological Process annotation using the High-Throughput GoMiner analysis tool (16). The GoMiner tool allows one to use Gene Ontology annotation classification categories to determine

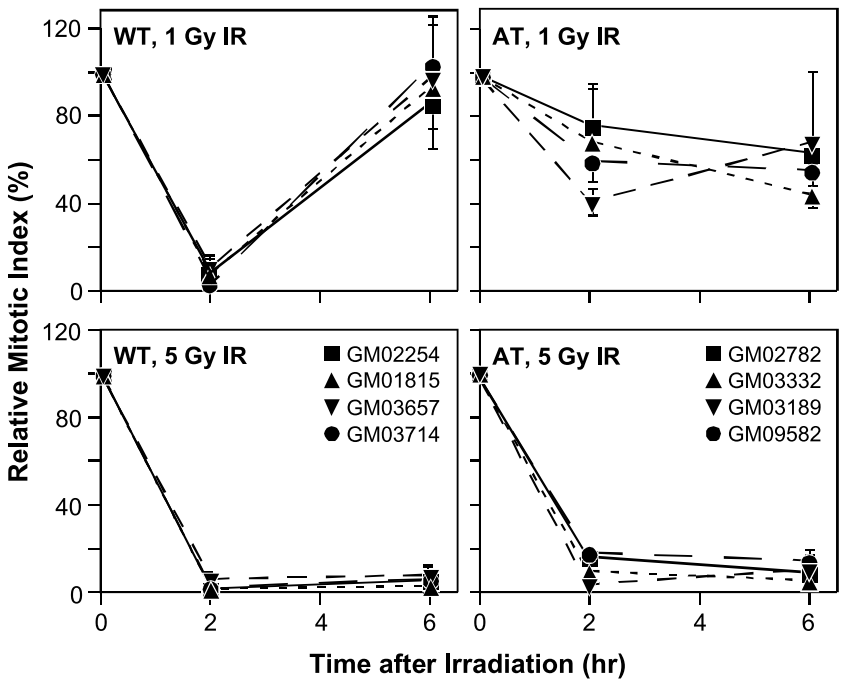

FIGURE 1. G_2 delay is attenuated in AT lymphoblast cells following exposure to 1 Gy but not 5 Gy IR. Exponentially growing cells were mock-treated or exposed to 1 or 5 Gy IR. Cells were harvested 2 or 6 hours after treatment and assayed for mitotic cells by flow cytometry by staining with phosphohistone H3 antibody. Points, mean relative mitotic indices (% mitotic cells in IR-treated cells/% mitotic cells in mock-treated cells); bars, SD. Experiments were done in triplicate.

overrepresentation of differentially expressed genes in a particular category with respect to the total number of genes represented in that category that are being measured with a particular platform.

The National Institute of Environmental Health Sciences Human ToxChip contains genes that were selected as being important in normal biological processes and responses to environmental stresses (17) and 1,606 of these genes were categorized into Gene Ontology categories. When these genes were categorized into Gene Ontology Biological Processes, the most represented processes included metabolism, cell cycle, and cell proliferation. Although we did find that some of the overrepresented processes determined for our treatment conditions (see below) were among the processes most highly represented on the chip, other processes that are also highly represented on the chip, such as transcription or localization, were not found to be significantly affected.

We identified the top 10 Biological Processes ranked by statistical significance of their $\log_{10}(P)$ value for each cell and treatment type. In the cases where the differential gene expression changes were robust (e.g., WT fibroblasts exposed to 5 Gy IR) all 10 categories had highly significant $\log_{10}(P)$ values. In these cases, only the top 10 $\log_{10}(P)$ values reflecting the most significant biological process classifications were used although there were other Biological Process classifications that had significant $\log_{10}(P)$ values. On the other hand, in those cases where the gene expression changes were more subtle (e.g., AT lymphoblasts exposed to 1 Gy IR), some of the $\log_{10}(P)$ values did not reach statistical significance but were used for comparative analysis. We combined all these into a single list of 36 categories. To more clearly visualize the Gene Ontology tree structure relationships, additional "parent" categories were added to bring the total to 46 categories. The additional parent categories are cellular process, cell communication, cellular physiologic process, regulation of cell proliferation, physiologic process, cell death, metabolism, cellular metabolism, cellular protein metabolism, and cellular biosynthesis. These categories do not change the results of the clustering (data not shown). $\text{Log}_{10}(P)$ values for each of these were then extracted from the individual analyses of each cell type and treatment group and compiled.

The resulting $\log_{10}(P)$ values from these categories from each of the individual cell cultures and treatment conditions were subjected to hierarchical clustering and certain similarities and differences were readily apparent on a very general level (Fig. 2). Specifically, there was a strong overrepresentation of differentially regulated genes in categories related to cell cycle, a classification that encompasses the progression of events that occur during cell replication or nuclear replication. In this area, WT lymphoblasts respond strongly to 5 Gy IR whereas WT lymphoblasts treated with 1 Gy IR and WT fibroblasts show a somewhat weaker but still significant response. Interestingly, whereas this response was lacking in the AT fibroblasts treated with 5 Gy IR and in the AT lymphoblasts treated with 1 Gy IR, the AT lymphoblasts treated with 5 Gy IR showed a significant response in these categories. The same trend exists in regulation of protein kinase activity. Another striking result (Fig. 2) was that of a significant overrepresentation of differentially expressed genes in the DNA metabolism/replication–related processes in WT fibroblasts treated with 5 Gy IR and WT lymphoblasts treated with 1 Gy IR, whereas the WT lymphoblasts treated with 5 Gy IR have stronger signaling in the regulation of cell cycle. These observations suggest more similarities in gene expression responses between fibroblasts treated with 5 Gy IR and lymphoblasts treated with 1 Gy IR than between the fibroblasts and lymphoblasts treated with the same dose of IR, both for WT and AT cultures. This suggested to us a potential role for an ATM-independent response contributing significantly in the lymphoblasts treated with 5 Gy IR, which we did not see in fibroblasts or lymphoblasts treated with 1 Gy IR (see below).

Comparisons of Cell Type–Specific Gene Expression Changes

We next looked at specific gene expression changes with respect to the cell type. Depending on the aspect of the cellular response examined, similarities and differences in differential expression of specific genes in the different cell types were observed. A similarity was seen in WT lymphoblasts and fibroblasts treated with 5 Gy IR in down-regulation of genes involved in mitosis (Table 1). Another similarity between cell types was seen in the down-regulation of DNA replication genes in all the WT cultures, whereas the AT cultures lacked this differential regulation of DNA replication genes (Table 1).

Similar patterns of up-regulation of DNA damage response genes and genes involved in apoptosis indicated little cell type–specific differential response following IR-induced DNA damage in the WT cultures (Table 1). However, there was a difference in the response of the AT cultures. The AT lymphoblasts treated with 5 Gy displayed an up-regulation of the same genes as the WT lymphoblasts [*CDKN1/p21/WAF1, Cyclin G1 (CCNG1), DDB2, GADD45A, PCNA, BAX*, and *FAS*], whereas the AT fibroblasts treated with 5 Gy showed a lack of differential regulation of most of these genes and the AT lymphoblasts treated with 1 Gy showed differential regulation of only some of these genes.

Comparisons of Dose-Specific Gene Expression Changes

Gene expression responses between lymphoblasts treated with 1 and 5 Gy IR were compared and found to differ. One striking difference between WT lymphoblasts treated with the two doses was the down-regulation of genes involved in cell cycle regulation [*cyclin A2* and *cyclin B1* (*CCNA2* and *CCNB1*), *CDKN3*, and *CKS2*] and mitosis (*CDC20, MAD2L1, KPNA2, NEK2*, and *STK6*) in cultures treated with 5 Gy IR but not following 1 Gy IR (Table 1).

WT lymphoblasts displayed similar levels of G_1 arrest after 1 and 5 Gy (35% and 43% inhibition, respectively). Consistent with similar levels of G_1 arrest is the similar down-regulation of DNA replication genes between 1 and 5 Gy–treated lymphoblasts. Similar responses were also seen in both DNA-damage response and apoptosis-related genes (*CDKN1A, CCNG1, DDB2, GADD45A, BAX*, and *FAS*), which were induced by both doses of IR in WT lymphoblasts, in agreement with previously published observations (18, 19). Changes in expression of genes in other biological pathways were also observed, with the WT lymphoblasts treated with 5 Gy IR displaying a greater trend of differential gene expression in response to the higher dose of DNA damage, as expected.

Table 1. Statistically Significant Differentially Regulated Genes in IR-Treated Lymphoblasts and Fibroblasts Classified into Functional Categories

Gene Symbol and Function	Clone ID*	Average of IR/Control Ratios †, ‡						Gene Name
		Lymphoblasts				Fibroblasts		
		WT (1 Gy)	AT (1 Gy)	WT (5 Gy)	AT (5 Gy)	WT (5 Gy)	AT (5 Gy)	
Cell cycle regulation								
CCNA2	32811	1.02	1.05	**0.66**§	0.96	**0.55**	1.03	*Cyclin A2*
CCNB1	563130	1.08	1.27	0.71§	0.77	0.98	1.12	*Cyclin B1*
CCNG1	321743	**1.48**§	1.16	**1.78**§	**1.75**§	**1.45**	1.35	*Cyclin G1*
CDC25B	179373	1.22§	1.05	0.82	0.92	0.86	1.21	*Cell division cycle 25B*
CDK10	310428	1.03	1.11	1.04	1.05	1.10	**0.38**	*Cyclin-dependent kinase (CDC2-like) 10*
CDKN1A	268652	**1.75**§	**1.52**§	**3.07**§	**2.55**§	**2.95**§	1.24§	*Cyclin-dependent kinase inhibitor 1A (p21, CIP1, WAF1)*
CDKN3	293274	1.07	1.02	0.78§	0.90	0.88	0.98	*Cyclin-dependent kinase inhibitor 3 (KAP)*
CKS2	359119	1.10	1.07	0.68§	**0.75**	1.14	1.20	*CDC28 protein kinase 2*
PLK3	324917	1.19	1.21	1.57	**1.58**	1.36§	1.12	*Polo-like kinase 3 (Drosophila; CNK, FNK, PRK)*
Mitosis								
CDC20	563809	1.14	1.02	**0.47**§	**0.55**	**0.52**§	1.16	*CDC20 cell division cycle 20 homologue (S. cerevisiae)*
KPNA2	339075	1.11	1.12	**0.52**§	0.80	0.84	1.02	*Karyopherin α2 (RAG cohort 1, importin α1)*
MAD2L1	129140	0.94	1.15	0.69§	0.94	**0.62**§	1.07	*MAD2 mitotic arrest deficient-like 1 (yeast)*
NEK2	415089	1.10	1.38	**0.57**§	**0.69**	0.65§	0.85	*NIMA (never in mitosis gene a)–related kinase 2*
STK6	415639	1.11	1.05	**0.71**§	0.95	**0.62**§	1.04	*Serine/threonine kinase 6 (STK15, Aurora 2, Aurora A)*
DNA replication								
CDC6	563187	**0.73**	1.07	0.77§	1.04	0.81	1.14	*CDC6 cell division cycle 6 homologue (S. cerevisiae)*
FEN1	49950	**0.73**	0.96	0.80§	1.08	**0.68**§	1.14	*Flap structure-specific endonuclease 1*
MCM2	358858	**0.76**	1.03	0.86	0.97	**0.66**	0.94	*MCM2 minichromosome maintenance deficient 2 (S. cerevisiae)*
MCM3	346838	**0.75**	0.98	**0.62**§	0.89	**0.63**§	0.97	*MCM3 minichromosome maintenance deficient 3 (S. cerevisiae)*
MCM4	130204	**0.70**§	1.00	**0.67**§	1.02	0.95	1.03	*MCM4 minichromosome maintenance deficient 4 (S. cerevisiae)*
MCM7	530696	**0.67**	1.04	0.96	1.17	**0.66**§	1.18	*MCM7 minichromosome maintenance deficient 7 (S. cerevisiae)*
MYC	417226	**0.70**§	0.92	**0.55**§	0.87	0.88	0.93	*v-Myc myelocytomatosis viral oncogene homologue (avian)*
PCNA	344109	1.03	1.10	**1.79**§	**1.75**§	**1.56**	1.25	*Proliferating cell nuclear antigen*
POLE	321207	0.92	0.97	0.95	1.07	**0.73**	1.01	*Polymerase ϵ*
RFC3	256260	0.96	1.11	0.91	1.04	**0.67**	1.17	*Replication factor C3*
RFC4	196676	**0.78**	1.04	0.92	1.10	**0.60**§	1.06	*Replication factor C4*
UNG	293111	**0.66**§	1.09	0.99	1.10	0.90	1.13	*Uracil-DNA glycosylase (UDG)*
Damage response/repair								
CCNG1	321743	**1.48**§	1.16	**1.78**§	**1.75**§	**1.45**	1.35	*Cyclin G1*
CDKN1A	268652	**1.75**§	**1.52**§	**3.07**§	**2.55**§	**2.95**§	1.24§	*Cyclin-dependent kinase inhibitor 1A (p21, CIP1, WAF1)*
DDB2	209321	**1.58**§	**1.33**§	**2.31**§	**1.96**§	**1.69**§	0.98	*Damage-specific DNA binding protein 2 (48 kDa)*
GADD45A	310141	**1.44**§	1.12	**1.80**§	**1.62**§	1.15	1.03	*Growth arrest and DNA-damage-inducible, α*
PCNA	344109	1.03	1.10	**1.79**§	**1.75**§	**1.56**	1.25	*Proliferating cell nuclear antigen*
Apoptosis								
BAX	869511	**1.58**§	1.19	**1.67**§	**1.68**§	1.21	1.16	*Bcl2-associated X protein*
CDKN1A	268652	**1.75**§	**1.52**§	**3.07**§	**2.55**§	**2.95**§	1.24§	*Cyclin-dependent kinase inhibitor 1A (p21, CIP1, WAF1)*
FAS	151767	**1.53**§	**1.25**	**1.79**§	**1.74**§	**1.57**	1.21	*TNF receptor superfamily, member 6 (APO1, TNFRSF6, CD95)*
TNFRSF10B	209683	1.17	1.43	1.63	1.60	**1.71**	0.98	*TNF receptor superfamily, member 10b (DR5, TRAILR2)*
TRAF2	510375	0.97	1.00	1.06	1.06	**0.71**	1.08	*TNF receptor–associated factor 2 (TRAP)*
Oxidation reduction/oxidative stress								
GPX1	415495	**1.32**§	1.04	**1.49**	**1.52**	1.10	1.31	*Glutathione peroxidase 1*
GSTT1	310535	**1.22**§	1.11	1.03	1.05	1.01	0.97	*Glutathione S-transferase θ1*
MGST1	292633	0.98	1.03	0.79§	0.90	0.96	0.92	*Microsomal glutathione S-transferase 1*
Protein metabolism/modification/transport								
CAMK1	429057	1.17	1.33§	1.11	1.00	0.95	0.99	*Calcium/calmodulin-dependent protein kinase I*
CTSD	264117	**1.39**§	**1.20**§	**1.93**§	**1.89**§	1.20	1.11	*Cathepsin D (lysosomal aspartyl peptidase)*
KIT	270882	1.09	1.10	1.42	1.00	0.92	**0.41**	*v-Kit Hardy-Zuckerman 4*
KPNA2	339075	1.11	1.12	**0.52**§	0.80	0.84	1.02	*Karyopherin α 2 (RAG cohort 1, importin α1)*
MAP3K8	109940	1.01	1.07	1.08	**1.57**	0.99	0.89	*Mitogen-activated protein kinase kinase kinase 8*
MDM2	147075	1.40	1.29	2.15	1.52§	1.27	1.02	*Mdm2, transformed 3T3 cell double minute 2, p53 binding protein (mouse)*
PPEF1	50472	0.93	1.13	0.68§	1.06	1.02	0.81	*Protein phosphatase, EF hand calcium-binding domain 1*
RPGR	469680	1.05	1.22§	1.14	1.04	0.92	1.02	*Retinitis pigmentosa GTPase regulator*
RPL27A	509719	1.04	1.06	1.16	1.01	1.01	1.23§	*Ribosomal protein L27a*
RPS6KA1	376362	1.16	1.06	**1.67**	**1.40**	1.02	1.06	*Ribosomal protein S6 kinase α1*
RSP19	550131	1.21§	1.05	1.25	1.18	1.07	1.10	*Ribosomal protein S19*

(*Continued on the following page*)

Table 1. Statistically Significant Differentially Regulated Genes in IR-Treated Lymphoblasts and Fibroblasts Classified into Functional Categories (Cont'd)

Gene Symbol and Function	Clone ID*	Average of IR/Control Ratios †, ‡						Gene Name
		Lymphoblasts				Fibroblasts		
		WT (1 Gy)	AT (1 Gy)	WT (5 Gy)	AT (5 Gy)	WT (5 Gy)	AT (5 Gy)	
RNA metasolism and processing								
CSTF3	417897	1.09	1.04	**1.71**	1.14	1.01	0.99	*Cleavage stimulation factor, 3′ pre-RNA, subunit 3*
DDX21	305307	**0.78**	0.95	**0.68**§	0.90	0.93	1.06	*DEAD/H (Asp-Glu-Ala-Asp/His) box polypeptide 21*
SFRS7	487937	0.88	0.98	0.79§	1.07	0.90	1.06	*Splicing factor, arginine/serine-rich 7 (35 kDa)*
Transcription								
CEBPD	82850	1.00	1.61§	0.85	0.96	1.06	1.03	*CCAAT/enhancer binding protein (C/EBP), δ*
CEBPG	612403	0.90	1.02	0.76§	0.91	0.89	0.96	*CCAAT/enhancer binding protein (C/EBP), γ*
ELF4	324210	0.87	0.98	0.77§	0.97	0.97	1.07	*E74-like factor*
IRF1	323001	1.03	1.05	**1.58**	1.10	1.00	1.05	*IFN regulatory factor 1*
MYC	417226	**0.70**§	0.92	**0.55**§	0.87	0.88	0.93	*v-Myc myelocytomatosis viral oncogene homologue (avian)*
TCEB3	249348	0.92	1.06	1.09	0.96	1.09	**0.44**	*Transcription elongation factor B(SIII), polypeptide 3 (110 kDa, elongin A)*
Neuronal								
GCH1	259642	1.15	1.12	**1.53**	1.19	0.98	0.96	*GTP cyclohydrolase 1*
LIF	153025	1.38	1.34	**2.00**§	1.15	1.12	0.87	*Leukemia inhibitory factor (cholinergic differentiation factor)*
RAB3A	163579	0.94	1.52	0.77§	1.03	1.15	0.96	*RAB3A, member RAS oncogene family, GTP-binding protein*
Signal transduction								
APBB3	279920	1.03	1.08	1.19	**1.45**	1.11	0.83	*Amyloid β (A4) precursor protein-binding, family B, member 3*
EPS8	415605	1.05	1.20§	1.10	1.23	1.06	1.09	*Epidermal growth factor receptor pathway substrate 8*
FGR	347751	1.20§	1.01	1.44	**1.41**	0.99	1.02	*Gardner-Rasheed feline sarcoma viral (v-fgr) oncogene homologue*
ITGA2	525246	1.44	1.17	1.03	0.99	**1.44**	0.96	*Integrin subunit α-2*
ITPR2	128020	1.09	1.16	**1.39**	**1.39**	1.03	0.91	*Inositol 1,4,5-triphosphate receptor, type 2*
LRP8	137995	0.97	1.20§	0.78	0.96	0.96	0.99	*Low-density lipoprotein receptor–related protein 8, apolipoprotein E receptor*
MAP2K6	366420	1.14	1.24§	1.43	1.06	0.97	1.01	*Mitogen-activated protein kinase kinase 6 (MKK6)*
PRKCB1	114378	0.95	1.05	0.77§	1.03	0.95	0.96	*Protein kinase C, β1*
PTH	322051	**0.77**	1.04	0.95	1.06	0.95	0.95	*Parathyroid hormone*
RAB33A	276508	0.98	0.98	**0.71**	0.90	1.06	1.02	*RAB33A, member RAS oncogene family, GTP-binding protein*
TANK	470672	1.07	1.05	**1.37**	**1.33**	1.00	0.93	*TRAF family member-associated nuclear factor-κB activator*
Immune response								
CD4	365647	0.99	0.90	1.16	**2.00**	1.09	1.10	*CD4 antigen (p55)*
DAF	310800	**1.26**	1.14	1.06	1.12	1.07	**0.57**	*Decay accelerating factor for complement (CD55, Cromer blood group system)*
EBI3	470012	1.08	0.99	**1.28**	1.11	1.05	1.01	*EBV induced gene 3*
FCGR2A	36074	1.02	1.04	**1.62**	1.20	1.00	1.00	*Fc fragment of IgG, low affinity IIa, receptor (CD32)*
IL1R1	138265	1.02	1.20§	0.89	0.91	0.88	1.12	*Interleukin 1 receptor, type I*
IL6ST	249704	0.99	1.28	1.39	1.26	1.60	**0.76**§	*Interleukin 6 signal transducer (gp130, oncostatin M receptor)*
IRF1	323001	1.03	1.05	**1.58**	1.10	1.00	1.05	*IFN regulatory factor 1*
LIF	153025	1.38	1.34	**2.00**§	1.15	1.12	0.87	*Leukemia inhibitory factor (cholinergic differentiation factor)*
TAP1	489288	1.08	0.94	**1.46**	1.10	1.25	1.05	*Transporter 1, ATP-binding cassette, subfamily B (MDR)*
TNFSF4	35326	1.21§	1.11	**1.83**§	**1.68**§	1.19	0.92	*TNF ligand superfamily, member 4 (GP34, OX40L, CD134L)*
Other								
AKAP1	510182	0.95	1.02	**0.75**	0.88	0.94	0.94	*A kinase (PRKA) anchor protein 1*
AMD1	328814	0.94	1.05	0.75§	0.86	0.89	1.27	*S-adenosylmethionine decarboxylase*
CSF1	124554	1.12	1.12	**1.69**§	**1.62**§	1.02	1.02	*Colony stimulating factor 1 (macrophage)*
CTGF	487513	1.14	1.92	1.29	0.91	1.10	**0.41**	*Connective tissue growth factor*
E2IG3	261284	0.95	1.01	0.75§	0.90	0.95	1.04	*Putative nucleotide binding protein, estradiol-induced*
EFEMP1	485875	1.30	2.03	0.99	0.90	0.99	**0.44**	*EGF-containing fibulin-like extracellular matrix protein 1*
EST	366880	1.05	1.29§	1.03	1.01	1.02	1.00	*EST*
EST	417285	1.12	1.32§	1.08	1.17	1.25	0.89	*EST*
GFM2	48425	**1.27**§	1.39	1.46	1.28	1.20	1.03	*G elongation factor, mitochondrial 2*
GPRP	530825	1.15	1.12	**1.41**	1.11	1.03	1.14	*Glutathione peroxidase–related protein*
GUK1	470177	1.03	1.09	1.04	1.03	1.09	1.24§	*Guanylate kinase 1*
HM74	123666	1.34§	2.02	1.67	1.09	1.37	0.92	*Putative chemokine receptor; GTP-binding protein*

(*Continued on the following page*)

Table 1. Statistically Significant Differentially Regulated Genes in IR-Treated Lymphoblasts and Fibroblasts Classified into Functional Categories (Cont'd)

Gene Symbol and Function	Clone ID*	Average of IR/Control Ratios †, ‡						Gene Name
		Lymphoblasts				Fibroblasts		
		WT (1 Gy)	AT (1 Gy)	WT (5 Gy)	AT (5 Gy)	WT (5 Gy)	AT (5 Gy)	
INSIG1	429092	0.97	1.08	0.77§	0.92	0.96	1.00	*Insulin-induced gene 1*
KNG1	195723	1.04	1.10	0.74§	0.82	1.29	0.91	*Kininogen 1*
LAMB1	509511	1.05	1.69	0.80§	0.90	1.09	1.12	*Laminin, β1*
LBR	307225	0.95	1.02	**0.60**§	0.97	0.84	1.04	*Lamin B receptor*
LMNB2	485332	0.86	0.95	0.94	0.90	**0.71**	1.09	*Lamin B2*
LRPAP1	376088	1.01	1.77	**1.62**	1.14	0.97	0.83	*Low-density lipoprotein receptor-related protein associated protein 1*
MLF2	486104	1.17	1.04	**1.75**	1.19	1.01	1.05	*Myeloid leukemia factor 2*
ODC1	510487	0.85	0.93	**0.65**§	0.86	1.01	1.15	*Ornithine decarboxylase 1*
PPP3CC	301976	1.02	1.20	0.80§	0.98	1.05	0.96	*Calcineurin A γ (protein phosphatase 3 (formerly 2B), catalytic subunit)*
PTP4A1	297595	1.10	1.20	**1.82**	**1.59**§	1.31	1.30	*Protein tyrosine phosphatase type IVA, member 1*
SPAG9	289236	1.08	1.27§	1.06	0.94	1.01	0.85	*Sperm associated antigen 9*
TCL1A	200018	0.98	1.03	0.75§	0.95	1.00	0.89	*T-cell leukemia/lymphoma 1A*
TRIP6	208190	1.21§	1.08	1.32	1.17	1.11	1.17	*Thyroid receptor interactor*

NOTE: *CCNG1, CDKN1A, IRF1, LIF, MYC*, and *PCNA* are listed in multiple categories.
*Clone ID number from the NIEHS Human ToxChip.
†Significance determined by MAPS, 90% confidence level, in at least 5 of 12 or 7 of 16 hybridizations with Z scores ≤3.5 and including reverse fluor labelings per treatment group, with SD ≤1.0; value shown is the mean of calibrated ratios of values found to be significant (bold, highlighted).
‡Significance determined by mixed linear model analysis using all hybridizations per treatment group, $P \leq 0.005$, fold change ≥1.2 or ≤0.8 (§, highlighted).

An unsupervised hierarchical cluster analysis of all cultures and treatments was done using the genes shown in Table 1. Figure 3 shows the resulting dendogram of the treatment groups. A striking feature of this dendogram is the separation of the WT and AT lymphoblasts treated with 1 Gy (A and B, respectively) compared with the inseparability of the WT and AT lymphoblasts treated with 5 Gy IR (C), again suggestive of an ATM-independent element in gene expression following 5 Gy IR. Because of this observation, the gene expression observations, the biological process observations and the lack of an ATM-dependent difference in the G_2 checkpoint response in lymphoblasts exposed to 5 Gy IR, we chose to concentrate on differential gene expression following 1 Gy in lymphoblasts and 5 Gy in fibroblasts to focus on ATM-dependent cellular responses to IR. Figure 4 shows a hierarchical cluster analysis of the 64 differentially expressed genes from lymphoblasts treated with 1 Gy IR and fibroblasts treated with 5 Gy IR.

ATM-Dependent Specific Gene Expression Responses

In our previous examination of differentially expressed genes in WT and AT fibroblasts following 5 Gy IR (10), DNA replication and repair genes (*MCM2, MCM3, MCM7, POLE, FEN1, RFC3*, and *RFC4*) made up a majority of the ATM-dependent gene set, being down-regulated in WT but not AT cells (also seen in Table 1; Fig. 4B). Down-regulation of genes involved in the progression through mitosis (*NEK2, CDC20, MAD2L1*, and *STK6*) was ATM dependent in WT fibroblasts (also seen in Fig. 4C) and up-regulation of genes involved in DNA damage response/repair and apoptosis (*DDB2, CCNG1, PCNA, FAS*, and *TNFRSF10B*) in WT fibroblasts appeared to be predominantly ATM-dependent (also seen in Fig. 4A and Table 1). Principal component analysis was used to identify the genes that contributed the most information to the separation of specific treatment groups (10). Genes that contributed the most in principal component analysis to discriminate WT from AT fibroblasts fell mainly into the categories of DNA replication (*FEN1, CDC6, RFC4*, and *MCM3*) and mitosis (*CDC20, MAD2L1*, and *CCNA2*; ref. 10).

Similar to fibroblasts, in lymphoblasts treated with 1 Gy IR, genes involved in DNA replication displayed an ATM-dependent response (Fig. 4B; Table 1). Expression of genes involved in apoptosis and DNA damage response/repair (*CDKN1A, CCNG1, DDB2, GADD45A*, *BAX*, and *FAS*) was predominantly ATM-dependent in lymphoblasts (Fig. 4A; Table 1). In contrast to fibroblasts, genes involved in mitosis did not show ATM dependence (Fig. 4C; Table 1). Principal component analysis showed that the DNA replication–related genes *MYC* and MCM4, the oxidative stress response gene GPX1, and the DNA damage response genes *DDB2, CCNG1*, and *GADD45A* were among the most discriminating genes between WT and AT lymphoblasts (data not shown).

Discussion

ATM is activated by DNA damage and participates in signal transduction cascades associated with cell cycle checkpoints and DNA repair through activation of a number of transcription factors, including TP53 (4) and E2F1 (20). One of the hallmarks of AT is a predisposition to B- and T-cell lymphoid cancers (21), which may indicate an increased sensitivity to DNA damage in lymphocytes in AT patients. Gene expression patterns from two human cell types, lymphoblasts, as a potential disease target tissue, and fibroblasts, a nontarget tissue, were compared to further understand the cellular mechanisms of ATM-dependent and ATM-independent responses to IR-induced DNA damage. Lymphoblasts were treated with two doses of IR to examine their responses to different extents of DNA damage.

In general, in both lymphoblasts and fibroblasts, one detects gene expression changes in response to IR that seem to be TP53 and ATM dependent and/or ATM independent. Gene expression responses to the increased dose of IR exposure seem to be dominated by quantitative differences and not qualitative differences. The transcriptional alterations in these studies are fairly subtle and require rigorous statistical approaches to discern biologically meaningful changes from background noise. Using conservative statistical approaches has the consequence that one most likely will exclude some biologically meaningful responses from analysis because they do not meet the statistical criteria. Between cell types, it seems that fibroblasts respond to 5 Gy IR similarly to lymphoblasts exposed to 1 Gy IR on the transcriptional level in a number of categories of responses, including DNA damage and repair and apoptosis. In these last two categories, lymphoblasts responded more strongly to 5 Gy IR than fibroblasts, and this response is predominately ATM independent, most likely mediated through ATM-related kinases, such as ATR. Although it seems that ATR functions together with ATM in general, the degree of ATR signaling relative to ATM signaling in response to IR is dose dependent. It is unclear if EBV-transformed lymphoblasts are simply more sensitive to DNA damage than fibroblasts and are programmed to elicit a more intense response to genomic insults or if the exposures actually elicit unequal DNA damage in the different cell types. Additional studies are required to resolve this issue.

These data are in agreement with the known defects in G_1 checkpoint responses in AT cells (22, 23), as indicated by ATM-dependent differential expression of genes involved in the regulation of progression through S phase in lymphoblasts and fibroblasts. In all of our treatment groups, we noted ATM-dependent gene expression responses in genes

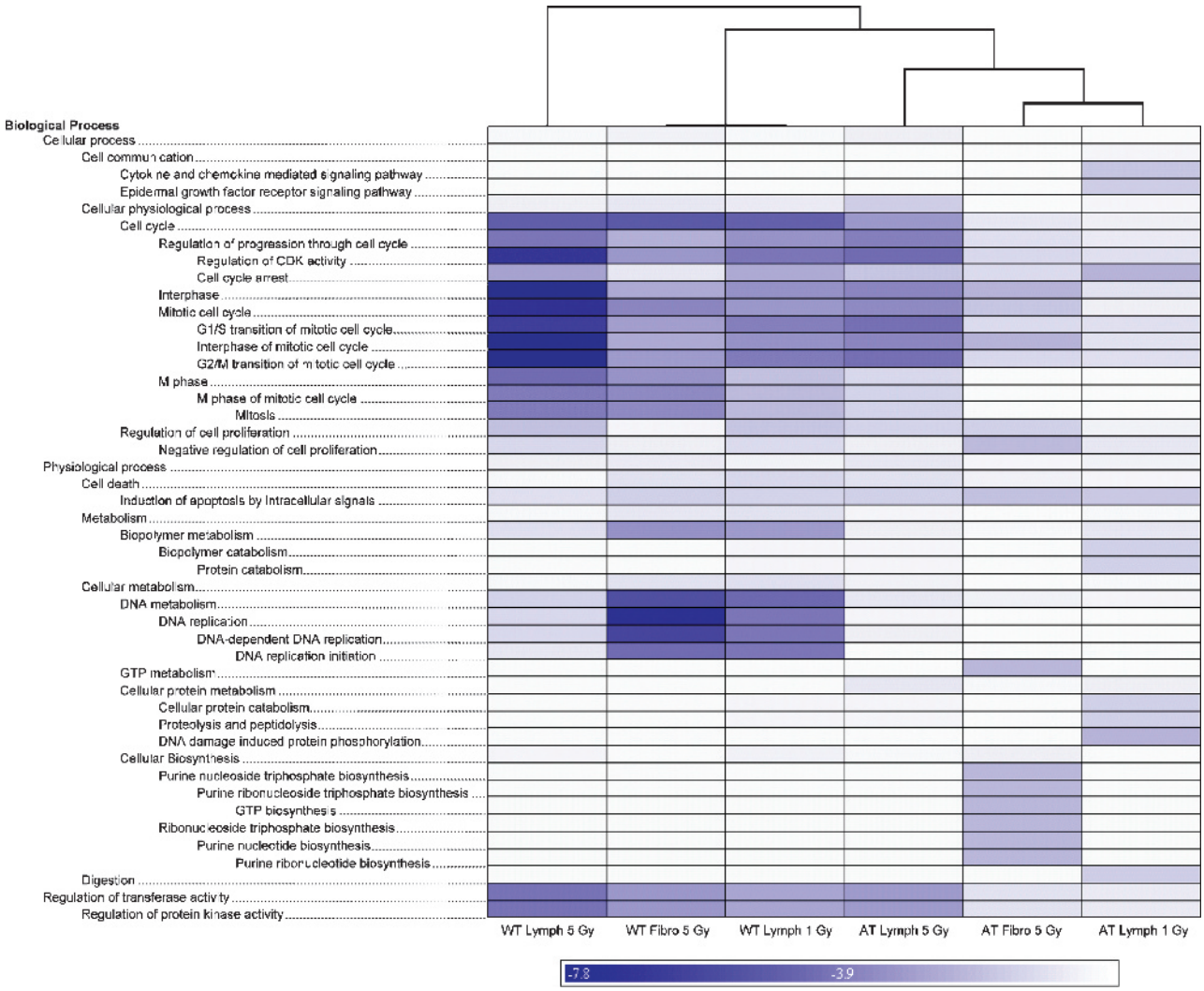

FIGURE 2. Genes determined to be differentially expressed (see Materials and Methods) were analyzed with respect to their Gene Ontology Biological Process annotation classifications using the GoMiner analysis tool. The top 10 Biological Process classifications, with respect to the significance of their $\log_{10}(P)$ values, were identified for each cell and treatment type. $\text{Log}_{10}(P)$ values for the top 10 Biological Processes for each treatment group were then subjected to unsupervised hierarchical cluster analysis of the cell and treatment groups based on a Pearson correlation of $\log_{10}(P)$ values and using average linkage grouping done with the Partek Pro 6.0 software program. Color bar, $\log_{10}(P)$ values.

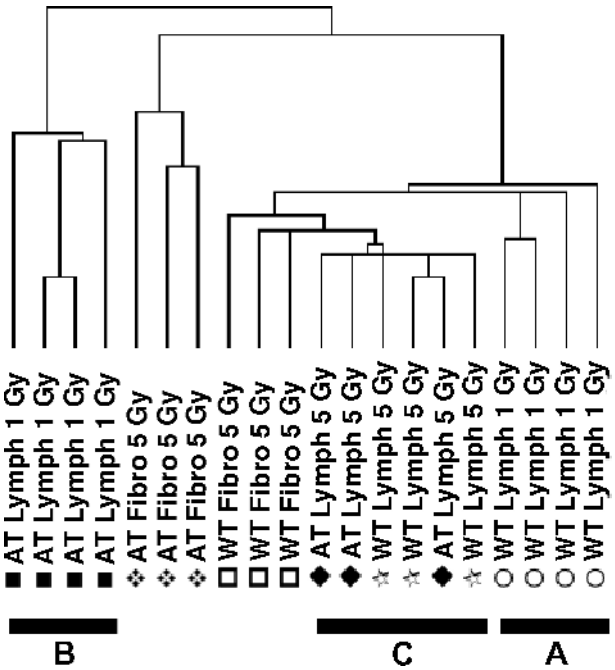

FIGURE 3. Dendogram of the relationship of all cultures based on gene expression patterns. The 102 differentially expressed genes listed in Table 1 were selected. Hierarchical cluster analysis was done on these genes, first clustering all of the genes and then the individual cell populations. The resulting information was converted into a cluster map in which the genes regulated most similarly (according to the correlation coefficient of their expression values) clustered together along the vertical axis and the most similar cultures clustered closest together along the horizontal axis. The length of the bars of the dendogram shows the relative similarity of the culture/treatments to each other with the shortest bars being the most similar in their gene expression patterns.

associated with DNA replication in one or more of the WT treatment groups but not in any of the AT treatment groups, thus discriminating between WT and AT cells in both cell types (Fig. 4B; Table 1).

AT cells are also known to have a defective early G_2 checkpoint response to IR (2, 22). Genes involved in G_2 checkpoint regulation and in progression through mitosis were generally down-regulated in an ATM-dependent manner in lymphoblasts and fibroblasts following 5 Gy IR. In the WT lymphoblasts, some of these genes were regulated in a dose-dependent manner following IR, with significant down-regulation following 5 Gy IR but not 1 Gy IR. This is in concordance with our G_2 checkpoint data where the G_2 checkpoint had been released by 6 hours following 1 Gy IR but not 5 Gy (Fig. 1). Histone H3 phosphorylation, as detected by flow analysis, also showed that AT lymphoblasts had an attenuated G_2 checkpoint response following 1 Gy IR, but exposure to 5 Gy IR resulted in an arrest in AT cells that was equivalent to that seen in WT cells. Interestingly, the AT lymphoblasts treated with 5 Gy IR, which were lacking cells in mitosis, did not show significant down-regulation of G_2 checkpoint and mitosis-associated genes. This likely reflects the reliance on posttranslational protein modifications to induce the G_2 checkpoint response to DNA damage. Although AT cells are defective in G_2 checkpoint response to IR-induced DNA damage, they nevertheless respond to IR with a, albeit attenuated, G_2 delay. The related checkpoint kinase ATR shares many substrates with ATM (24) and is known to contribute to cellular responses to IR (25). It is likely that differential gene expression changes and G_2 delay seen in AT lymphoblasts after treatment with 5 Gy occur through ATR signaling.

There are controversial reports of apoptosis in IR-treated AT cells (see ref. 26). Differential gene expression was observed for a number of apoptosis-related genes that were dose dependent in the lymphoblasts and ATM dependent in both cell types. Gene expression patterns in the lymphoblasts indicated some ATM-dependent regulation, which was overridden at the higher damage-inducing dose. Considerable interindividual variability was observed for differential expression of these genes, which might contribute to variation in apoptotic response. In addition, it is unclear how EBV is differentially affecting each of these lymphoblast cultures (27, 28). The mechanism whereby normal human fibroblasts resist radiation-induced apoptosis is not known, although studies suggest that basal levels of expression of CDKN1A/p21/Waf1 and GADD45 can influence whether cells arrest growth or undergo apoptosis when irradiated (29).

In summary, gene expression analysis has revealed responses to IR that are ATM dependent and are shared between lymphoblasts and fibroblasts (e.g., DNA replication and DNA damage and repair responses), responses that are predominately in one particular cell type (e.g., mitosis in fibroblasts and oxidative stress responses in lymphoblasts), and, at higher doses, ATM-independent responses that likely are dependent on signaling by ATR (e.g., DNA damage and repair and apoptotic responses in AT lymphoblasts following exposure to 5 Gy IR).

Materials and Methods

Cell Culture and Treatment

EBV-transformed lymphoblasts (National Institute of General Medical Sciences Human Genetic Mutant Cell Repository, Camden, NJ) from four normal (ATM WT) individuals (GM03714, GM02254, GM03657, and GM01815) and four individuals with AT (ATM-deficient; AT; GM03332, GM02782, GM09582, and GM03189) were maintained in RPMI supplemented with 15% FCS (Life Technologies, Inc., Grand Island, NY). Human dermal diploid fibroblasts described previously (10) were from three WT individuals (GM03349, GM08400, and GM08402) and three individuals with AT (GM02052, GM03395, and AG03058) and were used between passages 14 to 20. Cells were irradiated as previously described for 5 Gy (30) or at a rate of 0.9 Gy/min for a final dose of 1 Gy, then harvested 6 hours later for microarray analysis or as specified depending on further analysis.

Checkpoint Function

A flow cytometric method (13) was used to quantify the IR-induced reduction in the fraction of cells in the first quarter of S (2-2.5N DNA content) as a measure of G_1 checkpoint function (15). The percentage of lymphoblasts in mitosis was quantified by measurement of phosphorylated histone H3 (31), and the IR-induced reduction in mitotic cells was determined as a measure of G_2 checkpoint function.

RNA Preparation, cDNA Labeling, and Microarray Hybridization

Cells were harvested 6 hours following treatment, pelleted, and flash frozen. RNA isolation, cDNA generation, Cy3- or Cy5-dUTP labeling, hybridization to the National Institute of Environmental Health Sciences Human ToxChip, with ~1,901 cDNA probes for known genes and expressed sequence tags (http://dir.niehs.nih.gov/microarray/inhousearrays.htm), and analysis methods used were described previously (30). Four hybridizations, with fluor reversals, were done for each culture at each IR dose.

Statistical Analysis

Acquisition of the signal intensities, calibration of intensity ratio values, and identification of differentially expressed gene changes based on a confidence level approach (32) and an ANOVA mixed linear model approach (33) were done as previously described (30). Briefly, for the confidence level approach, digitized pixel intensity images generated by dual laser scanning of cDNA microarray chips hybridized with fluorescently labeled (Cy3 and Cy5) cDNA probes were analyzed with Array Suite v2.0 extensions of IPLabs image processing software (Scanalytics, Fairfax, VA). Pixel intensity values corresponding to each cDNA feature on the microarray chip from both scanning channels were adjusted by subtracting the local background surrounding each gene target. The ratio of the pixel intensity values for each gene target was normalized to all genes spotted on the chip to balance the two scanning channels to a ratio of ~1.0. Criteria for identifying a gene as significantly differentially expressed in lymphoblasts were set at the 90% confidence level and in at least 7 of 16 (1 Gy) or 5 of 12 (5 Gy) hybridizations with Z scores of ≤3.5, including reverse fluor labelings per treatment group and a SD of ≤1.0. For mixed linear model, $\log_2$-transformed, background subtracted pixel intensity values from each scanning channel were normalized to account for experiment-wide systematic effects by fitting the data with an ANOVA-mixed linear model consisting of an overall mean value, main fixed effects for the treatments and arrays, a random effect for the dye label, interaction effects of array and dyes, and random error. Residues from this normalization model were carried into a gene model with terms to account for overall intensity of each

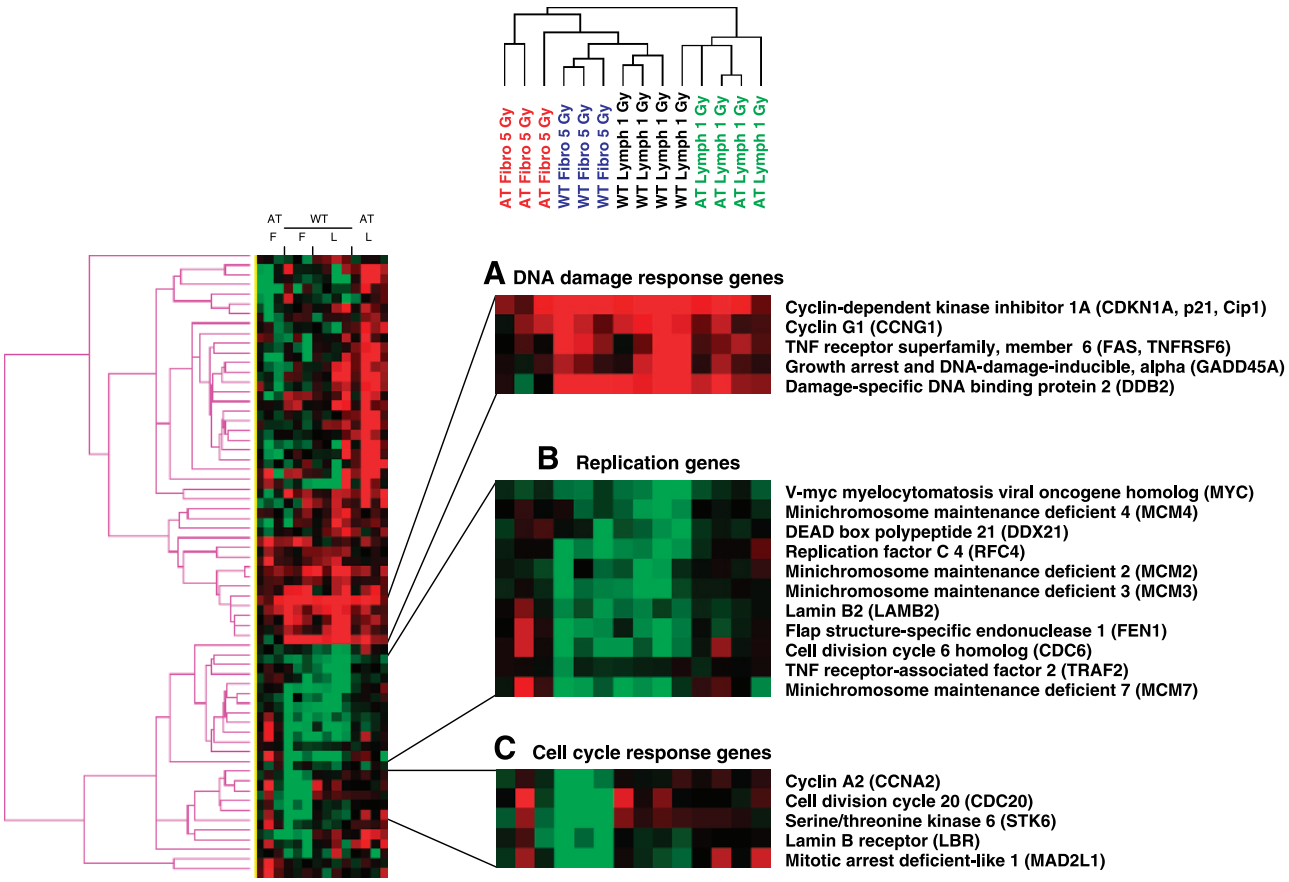

FIGURE 4. Cluster map of the 64 genes whose expression was significantly altered in irradiated lymphoblasts and fibroblasts. Genes that were differentially regulated in lymphoblasts following 1 Gy IR treatment and in fibroblasts following 5 Gy IR were combined, and a hierarchical cluster analysis that first clustered all of the genes and then the individual cell populations was done. The resulting information was converted into a cluster map. Each row corresponds to a single gene and each column corresponds to a single culture/treatment. The magnitude of the ratio of gene expression of treated versus untreated samples was converted into color intensity: red, highest ratio of expression (up-regulated); green, lowest level of expression (down-regulated). **A.** Cluster of genes associated with response to DNA damage. **B.** Cluster of genes associated primarily with DNA replication. **C.** Cluster of genes associated with cell cycle, primarily mitosis.

gene, treatment, and dye main fixed effects and an array random effect that measures the response of a gene to a given IR exposure in each cell type. Enrichments of Gene Ontology Biological Process annotations, based on the Nov 05 Unigene build for differentially expressed genes, were assessed using the software tool High-Throughput GoMiner (16). This software program calculates enrichment or depleting of functional categories by comparing the frequency of genes annotated to a particular process term from the list of differentially expressed genes versus that for the entire chip, using the two-sided Fisher exact test (34). The P value should be considered as a heuristic measure of probability of the observed annotation frequency to a functional category in the differentially expressed list being derived from the background frequency of the entire chip (16). Log_{10} of the P [$\log_{10}(P)$] values for the top 10 biological processes for each treatment group were then subjected to unsupervised hierarchical cluster analysis of the cell and treatment groups using Pearson correlation and average linkage grouping done with the Partek Pro 6.0 (St. Charles, MO) software program.

A two-dimensional gene expression data matrix with genes as the objects (rows) and sample treatments as the attributes (columns) was generated using the union set of genes that were differentially expressed in at least one of the cell and irradiation treatment groups and had a low probability ($P < 0.005$) of being randomly detected at the 90% confidence level (35). For each biological sample, the ratio intensity values for the differentially expressed genes were $\log_2$ transformed to approximate normality. Two-dimensional hierarchical cluster analysis was done using software and methods as described by Eisen et al. (36) with the following procedures to direct the agglomerative application. The Pearson correlation coefficient was used as a measure to determine similarity between gene expression vectors. Before clustering, the gene expression vectors were subjected to 1 million iterations of a self-organizing map to order the genes within clusters resulting in a smooth transition of gene expression patterns between clusters. The agglomerative clustering procedure was executed iteratively to merge similar gene expression vectors by measuring the Euclidian distance of a gene expression vector or cluster to all other gene expression vectors or clusters and then merging the two that were most similar.

Principal component analysis (37) was used to reduce the dimensionality of the ratio intensity data derived from the union set of differentially expressed genes and to identify the genes with the principal component loadings that contributed most to the separation of the treatment groups in multidimensional space.

Acknowledgments

We thank Drs. Douglas A. Bell and Bennett VanHouten, and Jianying Li for helpful comments.

References

1. Shiloh Y, Kastan MB. ATM: genome stability, neuronal development, and cancer cross paths. Adv Cancer Res 2001;83:209–54.

2. Paules RS, Levedakou EN, Wilson SJ, et al. Defective G_2 checkpoint function in cells from individuals with familial cancer syndromes. Cancer Res 1995;55:1763–73.

3. Falck J, Petrini JH, Williams BR, Lukas J, Bartek J. The DNA damage-dependent intra-S phase checkpoint is regulated by parallel pathways. Nat Genet 2002;30:290–4.

4. Banin S, Moyal L, Shieh SY, et al. Enhanced phosphorylation of p53 by ATM in response to DNA damage. Science 1998;281:1674–7.

5. Canman CE, Lim DS, Cimprich KA, et al. Activation of the ATM kinase by ionizing radiation and phosphorylation of p53. Science 1998;281:1677–9.

6. De la Torre C, Pincheira J, Lopez-Saez JF. Human syndromes with genomic instability and multiprotein machines that repair DNA double-strand breaks. Histol Histopathol 2003;18:225–43.

7. Gatti RA. The inherited basis of human radiosensitivity. Acta Oncol 2001;40:702–11.

8. Taylor AM. Chromosome instability syndromes. Best Pract Res Clin Haematol 2001;14:631–44.

9. Amundson SA, Bittner M, Fornace AJ, Jr. Functional genomics as a window on radiation stress signaling. Oncogene 2003;22:5828–33.

10. Heinloth AN, Shackelford RE, Innes CL, et al. ATM-dependent and -independent gene expression changes in response to oxidative stress, γ irradiation, and UV irradiation. Radiat Res 2003;160:273–90.

11. Cheung VG, Conlin LK, Weber TM, et al. Natural variation in human gene expression assessed in lymphoblastoid cells. Nat Genet 2003;33:422–5.

12. Correa CR, Cheung VG. Genetic variation in radiation-induced expression phenotypes. Am J Hum Genet 2004;75:885–90.

13. Shackelford RE, Innes CL, Sieber SO, Heinloth AN, Leadon SA, Paules RS. The ataxia telangiectasia gene product is required for oxidative stress-induced G1 and G_2 checkpoint function in human fibroblasts. J Biol Chem 2001;276:21951–9.

14. Kaufmann WK, Heffernan TP, Beaulieu LM, et al. Caffeine and human DNA metabolism: the magic and the mystery. Mutat Res 2003;532:85–102.

15. Kaufmann WK, Schwartz JL, Hurt JC, et al. Inactivation of G_2 checkpoint function and chromosomal destabilization are linked in human fibroblasts expressing human papillomavirus type16 E6. Cell Growth Differ 1997;8:1105–14.

16. Zeeberg BR, Qin H, Narasimhan S, et al. High-throughput GoMiner, an "industrial-strength" integrative gene ontology tool for interpretation of multiple-microarray experiments, with application to studies of Common Variable Immune Deficiency (CVID). BMC Bioinformatics 2005;6:168.

17. Afshari CA, Nuwaysir EF, Barrett JC. Application of complementary DNA microarray technology to carcinogen identification, toxicology, and drug safety evaluation. Cancer Res 1999;59:4759–60.

18. Amundson SA, Do KT, Shahab S, et al. Identification of potential mRNA biomarkers in peripheral blood lymphocytes for human exposure to ionizing radiation. Radiat Res 2000;154:342–6.

19. Akerman GS, Rosenzweig BA, Domon OE, et al. Alterations in gene expression profiles and the DNA-damage response in ionizing radiation-exposed TK6 cells. Environ Mol Mutagen 2005;45:188–205.

20. Lin WC, Lin FT, Nevins JR. Selective induction of E2F1 in response to DNA damage, mediated by ATM-dependent phosphorylation. Genes Dev 2001;15:1833–44.

21. Shiloh Y. Ataxia-telangiectasia and the Nijmegen breakage syndrome: Related disorders but genes apart. Annu Rev Genet 1997;31:635–62.

22. Beamish H, Lavin MF. Radiosensitivity in ataxia-telangiectasia: anomalies in radiation-induced cell cycle delay. Int J Radiat Biol 1994;65:175–84.

23. Khanna KK, Beamish H, Yan J, et al. Nature of G_1/S cell cycle checkpoint defect in ataxia-telangiectasia. Oncogene 1995;11:609–18.

24. Kim ST, Lim DS, Canman CE, Kastan MB. Substrate specificities and identification of putative substrates of ATM kinase family members. J Biol Chem 1999;274:37538–43.

25. Cliby WA, Roberts CJ, Cimprich KA, et al. Overexpression of a kinase-inactive ATR protein causes sensitivity to DNA-damaging agents and defects in cell cycle checkpoints. EMBO J 1998;17:159–69.

26. Vit JP, Moustacchi E, Rosselli F. ATM protein is required for radiation-induced apoptosis and acts before mitochondrial collapse. Int J Radiat Biol 2000;76:841–51.

27. Takahashi T, Kawabe T, Okazaki Y, et al. *In vitro* establishment of tumorigenic human B-lymphoblastoid cell lines transformed by Epstein-Barr virus. DNA Cell Biol 2003;22:727–35.

28. Sugimoto M, Tahara H, Ide T, Furuichi Y. Steps involved in immortalization and tumorigenesis in human B-lymphoblastoid cell lines transformed by Epstein-Barr virus. Cancer Res 2004;64:3361–4.

29. Canman CE, Gilmer TM, Coutts SB, Kastan MB. Growth factor modulation of p53-mediated growth arrest versus apoptosis. Genes Dev 1995;9:600–11.

30. Heinloth AN, Shackelford RE, Innes CL, et al. Identification of distinct and

common gene expression changes after oxidative stress and γ and ultraviolet radiation. Mol Carcinog 2003;37:65–82.

31. Deming PB, Flores KG, Downes CS, Paules RS, Kaufmann WK. ATR enforces the topoisomerase II-dependent G_2 checkpoint through inhibition of Plk1kinase. J Biol Chem 2002;277:36832–8.

32. Chen Y, Kamat V, Dougherty ER, Bittner ML, Meltzer PS, Trent JM. Ratio statistics of gene expression levels and applications to microarray data analysis. Bioinformatics 2002;18:1207–15.

33. Wolfinger RD, Gibson G, Wolfinger ED, et al. Assessing gene significance from cDNA microarray expression data via mixed models. J Comput Biol 2001;8: 625–37.

34. Zeeberg BR, Feng W, Wang G, et al. GoMiner: a resource for biological interpretation of genomic and proteomic data. Genome Biol 2003;4:R28. Epub 2003 March 25.

35. Bushel PR, Hamadeh HK, Bennett L, et al. Computational selection of distinct class- and subclass- specific gene expression signatures. J Biomed Inform 2003;35:160–70.

36. Eisen MB, Spellman PT, Brown PO, Botstein D. Cluster analysis and display of genome-wide expression patterns. Proc Natl Acad Sci U S A 1998; 95:14863–8.

37. Johnson DE. Applied multivariate methods for data analysts. New York: Duxbury Press; 1998.

Molecular Cancer Research

ATM Requirement in Gene Expression Responses to Ionizing Radiation in Human Lymphoblasts and Fibroblasts

Cynthia L. Innes, Alexandra N. Heinloth, Kristina G. Flores, et al.

Mol Cancer Res 2006;4:197-207.